International Journal of Power Electronics and Drive System (IJPEDS)
Vol. 17, No. 1, March 2026, pp. 282~292
ISSN: 2088-8694, DOI: 10.11591/ijpeds.v17.i1.pp282-292

An efficient grid-connected solar PV system with a fault-tolerant mechanism to mitigate the voltage disturbances

N. Jayakumar[1], B. Devi Vighneshwari[1], V. Prema[2]
[1]Department of Electrical and Electronics Engineering, The Oxford College of Engineering, affiliated to Visvesvaraya Technological University, Belagavi, India
[2]Department of Electrical and Electronics Engineering, B.M.S. College of Engineering, Bengaluru, India

Article Info

Article history:

Received Jul 24, 2025
Revised Nov 10, 2025
Accepted Dec 11, 2025

Keywords:

Dynamic voltage restorer
Fault-tolerant
Grid-connected system
Solar PV
Voltage disturbances

ABSTRACT

One of the most effective renewable energy solutions for long-term power generation is a solar photovoltaic (PV) system that is connected to the grid. However, power quality and system reliability can be significantly impacted by grid-side voltage disturbances such as sag, swell, and faults. To reduce voltage fluctuations and improve grid stability, this study proposes an effective fault-tolerant (FT) solar PV system coupled with a dynamic voltage restorer (DVR). The adaptive DVR-based control method, which dynamically injects compensatory voltages based on disturbance amplitude to ensure uninterrupted and distortion-free power delivery, is the feature that makes this study unique. MATLAB/Simulink is used to model and simulate the system to assess its dynamic response under fault, sag, and swell situations. IEEE 519 standards are met by the suggested design, which produces average total harmonic distortion (THD) values of 0.59%, 1.16%, and 1.55% for 50%, 100% sag/swell, and three-phase fault circumstances, respectively. This indicates that even in challenging grid situations, the DVR can sustain high-quality voltage profiles. For implementation in renewable-rich or weak grid networks, the suggested FT-DVR configuration provides a workable and affordable solution that guarantees better voltage regulation, less harmonic distortion, and increased operational dependability for upcoming smart-grid integration.

Corresponding Author:

N. Jayakumar
Department of Electrical and Electronics Engineering
The Oxford College of Engineering, affiliated to Visvesvaraya Technological University
10th Milestone, Hosur Rd, Bommanahalli, Bengaluru, Karnataka 560068, India
Email: jayakumar.toce@gmail.com

1. INTRODUCTION

Fossil fuels, which are indeed limited, are used to create about 60% of the worldwide power supply [1]. By releasing carbon dioxide, carbon monoxide, and other harmful chemicals, they also hasten air pollution and global warming. On the other hand, solar energy is regarded as a plentiful and clean option. A significant amount of renewable energy is generated by solar photovoltaics. By 2028, solar photovoltaic (PV) and wind deployments are predicted to have more than doubled in size from 2022. Throughout the projection period, these forms of renewable power are expected to continuously beat historical records, eventually achieving an estimated capacity of around 710 GW [1], [2]. Advanced distribution systems (DSs) incorporate renewable energy sources (RESs) like wind, solar PV, hydropower, and biofuels innovations. Improved overall performance, decreased environmental impacts, migration to smaller MGs based on RES, and fewer costs for machinery due to shorter transmission lengths are just a few advantages of this integration.

Additional advantages of incorporating distributed generators (DGs) into the networks include responding to demand, handling energy, regional generation, constant power availability, and sustaining voltage [3].

DG units powered by renewable energy are linked to two different kinds of harmonics. Power electronics (PE) included in RESs produce the first kind of harmonics. An interface PE inverter is used to connect some forms of RESs, such as PV systems, to the grid. These inverters produce harmonics at the DG's output due to the PE components' switching. The structure's nonlinear local, point of common coupling (PCC), and utility loads at more than one of the power grid frequency ranges produce the second kind of harmonics. Utility providers must maintain the harmonics intensity at the PCC with every user within allowable bounds as mandated by grid rules to guarantee high-quality power delivered to the users [4]. Harmonics related to interacting inverters and their complex grid interaction necessitate additional investigation in this specific area due to the growing integration of RESs, including PV systems, into today's power networks [5]. To preserve power quality (PQ) in the grid that interfaces with solar energy production equipment, numerous global regulations exist. To ensure PQ and successfully mitigate PQ difficulties, the impact of distortions and inter-harmonics on transmission feeder voltage abnormalities is examined to meet IEEE requirements for distribution feeder electrical currents. A smart and innovative control mechanism must be developed for the solar energy system, which is interfaced with the grid system [6].

The three-phase current source inverters (CSI) without a transformer can benefit from a straightforward technique for mitigating ground leakage current [7]. The high voltage level at the standard direct current (DC) bus is achieved via a Kalman-based maximum power point tracking (MPPT) method with an intelligent current regulator for the grid-interfacing voltage source inverter (VSI) and maximum-gain DC–DC converter [8]. The construction of a basic single-phase grid-connected PV inverter uses a dynamic harmonic compensation mechanism for lower-order harmonic adjustment [9]. The powerful current controller is used to investigate the process of the harmonic current injected from grid-dependent single-phase inverter structures on single-phase solar power systems [10]. To enhance power quality and withstand voltage fluctuations, there are numerous mitigation strategies. To enhance the PQ of on-grid PV systems, the Trans-Z-source inverter-based dynamic voltage restorer (DVR) powered by solar PV was created [11]. For a multipurpose dual-stage grid-dependent solar PV system, an effective enhanced complicated Kalman filter-based controller is used to achieve this under unusual grid circumstances [12]. To mitigate fault-induced delayed voltage recovery (FIDVR), a day-and-night controller known as PV-static synchronous compensator (STATCOM) was built for an extensive PV solar field. This method works just as well as a STATCOM attached locally at motor loads and strengthens motors at night, which is above and beyond grid code standards [13].

The sustainability, affordability, and adaptability of grid-connected solar PV systems have made them one of the most promising renewable energy sources. Unstable power generation results from their performance being greatly impacted by changes in ambient temperature and solar irradiation. When connected to grid disruptions like faults, swells, and voltage sags, these variations deteriorate power quality and compromise the entire grid network's dependability. Dynamic fault events frequently cause harmonic distortion and non-compliance with IEEE power quality regulations due to the inability of current control methods and compensating procedures to maintain constant voltage regulation. In order to maintain grid stability and guarantee high-quality power delivery, a fault-tolerant grid-connected solar PV system that can dynamically compensate for voltage disruptions is essential.

A DVR is incorporated into the current work's fault-tolerant and efficient grid-connected solar PV system to efficiently mitigate grid-side voltage disturbances like sag, swell, and fault circumstances. For stable operation and optimal power extraction, the system uses a 200 W Waaree Energies WSM-315 PV module that is modelled using a perturb and observe (P&O) MPPT controller and a VSC-based average converter. To preserve voltage stability and improve power quality, the DVR dynamically injects compensatory voltages between the grid and the load. The suggested FT-DVR configuration significantly reduces total harmonic distortion (THD), as demonstrated by simulation results obtained in MATLAB/Simulink. The proposed work achieves better THD under various sag/swell/fault conditions and also within the IEEE 519 standard limits. All things considered, this work offers a strong, dependable, and cost-effective fault-tolerant solution for enhancing PQ and voltage management in grid-connected renewable energy systems. The organization of the paper is as follows: i) The proposed work is discussed in section 2; ii) The results and discussion of the grid-connected solar PV system, including simulation results, are highlighted in section 3; and iii) Lastly, the overall work is concluded in section 4 with a futuristic scope.

This section discusses the related work of the grid-connected solar PV system and its related techniques. In contrast to the traditional IEEE Std. 1547 VV-C techniques, Lee *et al.* [14] developed an enhanced Volt/VAR curve (VV-C) based control for dynamic VAR compensators (DVCs), achieving lower voltage variance. A three-phase, three-wire grid-integrated PSC-WECS architecture using a two-level voltage source converter managed by a polynomial zero-attracting least mean square (PZA-LMS) algorithm was introduced by Nazir *et al.* [15]. Their findings showed that improved converter-based designs are economically viable, as evidenced by 72% lower energy generation costs and a 50% decrease in physical

footprint. Advanced control techniques have been investigated to improve dynamic efficiency and power quality. The barrier function-based sliding mode control (BFSMC), which was introduced by Bagherwal and Mahapatra [16], performed better in preserving DC bus voltage stability than conventional proportional integral derivative (PID) and Lyapunov-based controllers. Model predictive control (MPC) operations can be made simpler with Bana *et al.* [17]'s artificial neural network (ANN)-based control technique, which greatly reduces computing complexity without sacrificing accuracy. Utilizing a control hardware-in-the-loop (C-HIL) configuration, they confirmed the ANN-based controller's dependability in real time. Comparing artificial intelligence to conventional deep learning techniques, Hassan *et al.* [18] showed better prediction accuracy and dependability when assessing PV system performance using operational and environmental information.

Fault tolerance and hybrid renewable integration have been the focus of subsequent developments. In order to provide stable operation during grid faults and weak-grid circumstances, Radwan *et al.* [19] designed a grid-forming voltage-source inverter (VSI) with direct current management for hybrid wind-solar converters. In their study of DC voltage control strategies for virtual synchronous machine (VSM) systems, Guo and Wu [20] emphasized the vulnerability of grid-forming inverters to voltage failure during variations in irradiance. For PV–wind hybrid systems, Mohamed *et al.* [21] used an adaptive neuro-fuzzy inference system (ANFIS) controller, which enhanced power quality and guaranteed steady grid integration. To improve grid synchronization and reactive power regulation, Sridhar *et al.* [22] developed a modular neural network (MNN)-based PI controller that dynamically adjusted gains in real time, lowering steady-state error by 45% and THD by 30%. Karimi and Sedigh [23] created a two-stage, five-level H-bridge inverter to reduce switching losses and harmonic distortion. Under normal circumstances, the THD values were 1.18%, while under partial shading, they were 3.01%. A hybrid decoupled and mid-point clamped architecture was presented by Kibria *et al.* [24] to lower leakage current while preserving steady power injection under closed-loop model predictive control (MPC). An adaptive harmonic reduction method called Atomic Orbital Search with feedback artificial tree (AOS-FAT) was introduced by Kiruthiga *et al.* [25] and achieved 1.1% THD and 12 kW PV output power. Wesseling *et al.* [26] examined the effects of integrated PVs, heat pumps, and EVs on grid imbalance; they found that under high renewable penetration, the imbalance may reach 15%. A modular high-voltage gain converter that considerably reduces switch stress was proposed by Bhaskar *et al.* [27]. In experimental validation, the converter achieved a 48–650 V conversion with 500 W output.

Despite increasing efficiency, most of these methods concentrate more on harmonic mitigation or converter control than on entire fault-tolerant functioning under dynamic voltage disturbances. A research gap still exists in the development of an integrated grid-connected solar PV system with a DVR to actively mitigate fault, sag, and swell conditions while adhering to IEEE 519 power quality protocols. By employing DVR to design and simulate an effective fault-tolerant grid-connected solar PV system, the current work fills this gap by improving grid voltage stability and reliability under a variety of disturbance situations.

2. METHOD

Figure 1 illustrates the proposed grid-connected solar PV system with the FT technique that uses a DVR. A 200 W solar PV array unit, DC to DC converters, a bridge inverter based on a voltage source converter (VSC), a VSC control procedure, an FT employing a DVR technique, and a three-phase load are the key components of the system. The PV system from solar energy functions as a grid system. Set the temperature and irradiance for the two solar array panels that are attached to the DC-DC converter initially. The perturb and observe (P&O) technique is used by the DC-to-DC converter, an active boost converter, to monitor the maximum power point (MPP) of PV arrays.

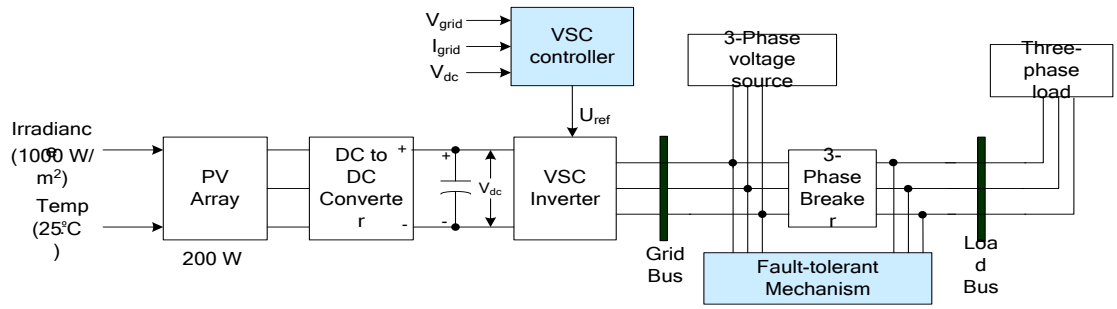

Figure 1. Proposed grid-connected solar PV system with a fault-tolerant mechanism

Both positive and negative connections are made between the DC-link capacitor and the DC-to-DC converter terminals. The inverter's VSC unit is used to create the reference gate signals (Uref). The utility grids or load-connected system's reactive current is compensated for by the VSC unit, which supplies the VSC current through the VSC inverter. By employing the VSC unit, the PV system and the load bus regulate the voltage synchronization. 12.66 kV is supplied to the grid bus by the three-phase programmable source or substation. Implementing a DVR module, the FT process compensates for fault and sag/swell concerns by connecting across the grid system and load bus. The DVR and load bus are connected to a three-phase breaker to create the sag/swell and fault circumstances. The Sag/Swell circumstances are provided by the three-phase programmable voltage sources, which change their amplitude during the duration of the simulation.

2.1. VSC-based inverter with control mechanism

Figure 2 illustrates the VSC process for the VSC-based inverter in the suggested design. In addition to providing the reference gate signals to the VSC-based inverter and preserving voltage coordination between the solar PV arrays and the load bus system, the VSC control structure is an efficient control method in the solar PV system. The PI-based feed-forward current (FCC) regulator, Park (abc to dq0) conversion, phase-locked loop (PLL), modulation index computation, and reference signal processing unit are all features of the VSC control unit. 500 V is the standard DC voltage (V_{dc_r}). Before the VSC control operation begins, the reference q-axis current (I_{q_r}) is set to zero. The angle and frequency data needed for the conversion procedure are supplied by the PLL.

The park conversion unit receives the three-phase synchronized pulses from the PLL via grid voltages (V_{grid}). The voltage and current signals generated by this unit are fed into the current regulator and are based on the direct (d) and quadrature (q) axes. A PI-based Vdc regulator is used to create the direct axis current. Employing dq voltages and currents, the current regulator generates both active and reactive power. The modulation index is further determined using the dq voltages. The reference gate signals to the VSC-based inverter are located using this modulation index.

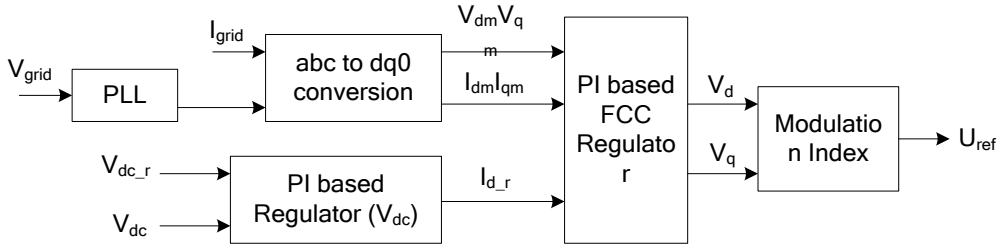

Figure 2. VSC controller for the VSC-based inverter in the proposed system

2.2. Fault-tolerant mechanism using DVR technique

The FT-based DVR technique takes into account the amplitude, frequency, and phase between the load bus unit and the grid system to deliver the injection voltage (i.e., maximum or minimum). Figure 3 depicts the DVR technique based on FT. Two-level converter, three-phase transformer, PI controller, LC filter, and pulse width modulation (PWM) generation unit are all included. After being contaminated by sag/swell or faults from the three-phase source, the input signals are sent to the three-phase transformer. For the PWM generator, the controller generates the controlled dq-axis voltage. Gate signals come from a PWM generator.

The load voltage is input to the conversion unit. The angle (θ) to both conversion units (dq0 to abc and abc to dq0) is generated by the discrete PLL. Deducting the reference dq voltage from the transformation's result (abc to dq0) yields the error signal. The reference dq voltages have been configured to '0' for the q-axis voltage and '1' for the d-axis voltage. After receiving the error signal, the PI controller responds with the controller result. For the d-axis and q-axis voltage response generation, the PI is utilized separately. After receiving the response results, the dq0 to abc conversion supplies the PWM generator with the correct three-phase voltage. The PWM sends the gate signals to the 2-level converter, which is subsequently linked to the DC supply. 500 V is the DC supply's setting. The PWM generator sends the gate signals (which serve as a reference input) to the two-level generator, which then produces the AC power. The necessary voltage (injected) is stored by the LC filter utilizing the 2-level converter and supplied as a corrected output voltage to the three-phase transformer. To address the sag/swell problems, this corrected voltage is further utilized in the load system. The LC filter stores the corrected voltage using low capacitance (20 µF) and inductance (10 mH) values.

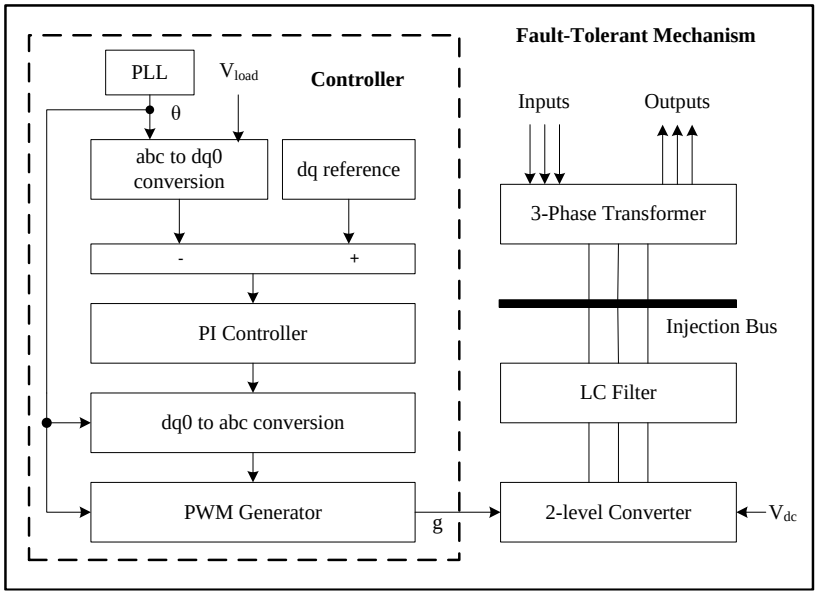

Figure 3. Proposed fault-tolerant mechanism using the DVR technique

3. RESULTS AND DISCUSSION

This section discusses the outcomes of the grid-connected solar PV system with the FT mechanism. In grid-connected solar PV systems, the DVR technique with a PI controller is utilized separately to adjust for faults and sag/swell. A PI controller is used to inject the DVR voltages to correct for the faults and sag/swell. In a three-phase programmable voltage source model, the amplitude variable is altered at a certain time to generate the sag/swell. To investigate the fault situations, the three-phase programmable voltage source model is replaced by the three-phase fault model. To produce the functional findings, the simulation time was set at 0.2 seconds. Throughout the design instances, the sag/swell or faults appear between 0.06 and 0.12 seconds.

In this work, a solar PV model is the Waaree Energies WSM-315 module. The following is a list of the solar PV system specifications: At its peak, the solar PV system will provide 315 W of power. To calculate power, a PV voltage of 35 V and a current of 9 A are established. The design specifies 72 cells per module, 43 V for the open circuit voltage, and 9.77 A for the short circuit current. Solar PV output is calculated by taking into account the light-generated current of 9.7966 A, the series resistance of 0.31273 Ω, and the shunt resistance of 115.0566 Ω. The 50% and 100% sag/swell conditions are introduced in the simulation between 0.06 and 0.12 seconds. Table 1 shows the results of the voltage study utilizing a grid-connected solar PV system with an FT mechanism under sag/swell situations. Before the sag/swell state, the grid voltage is set to 1 Vpu.

When there is no sag/swell, the grid voltage is set to 1 Vpu. 0.5 Vpu and 0 Vpu are the grid voltages under 50% and 100% sag situations, respectively. For 50% and 100% swell conditions, the grid voltages are also adjusted to 1.5 Vpu and 2 Vpu, respectively. Under no-sag/swell conditions, the produced load voltage is comparatively high, and as the percentage of sag/swell conditions rises, it significantly drops.

Figure 4 illustrates the simulation outcomes for the grid-connected solar PV system using FT mechanism under sag/swell conditions. At 50% sag situation, the load's voltage profile is approximately 0.992 Vpu, while the injected voltage is 0.049 Vpu. Likewise, the load's voltage profile is around 1.001 Vpu, while the injected voltage's profile is 0.049 Vpu under 50% swell conditions. Figure 4(a) displays the grid voltage, load voltage, and injected voltages under the 100% sag situation. When the injected voltage is at 100% sag, the load's voltage profile is approximately 0.999 Vpu and 0.0999 Vpu. Likewise, Figure 4(b) displays the grid voltage, load voltage, and injected voltages for the 100% swell condition scenarios. At 100% swell situation, the load's voltage profile is around 1.002 Vpu, while the injected voltage is 0.0996 Vpu.

Table 1. Voltage analysis at sag/swell conditions

Voltages (Vpu)	Sag		Swell	
	50%	100%	50%	100%
Grid voltage	0.5	0	1.5	2
Load voltage	0.992	0.999	1.001	1.002
Injected voltage	0.049	0.0999	0.049	0.0996

Table 2 presents the percentage THD computation of the load voltage for the DVR procedure under various conditions. When there is no sag or swell, the typical percentage THD of the load voltage is approximately 0.01. At 50% sag/swell, the average percentage THD of the load voltage is around 0.59, and at 100% sag/swell, it is 1.16. When there is no sag or swell, the average percentage THD of load voltage is low; when there is 100% sag or swell, the THD is larger. The fault between phases A, B, and C and the ground is created by the three-phase fault model. Individual faults between phases (A, B, C, AB, BC, AC, or ABC) and ground are discussed. Table 3 presents the voltage and THD evaluation of the suggested system under different fault scenarios. Figure 5 illustrates the simulation outcomes of the grid-connected solar PV system employing the FT mechanism under various fault scenarios.

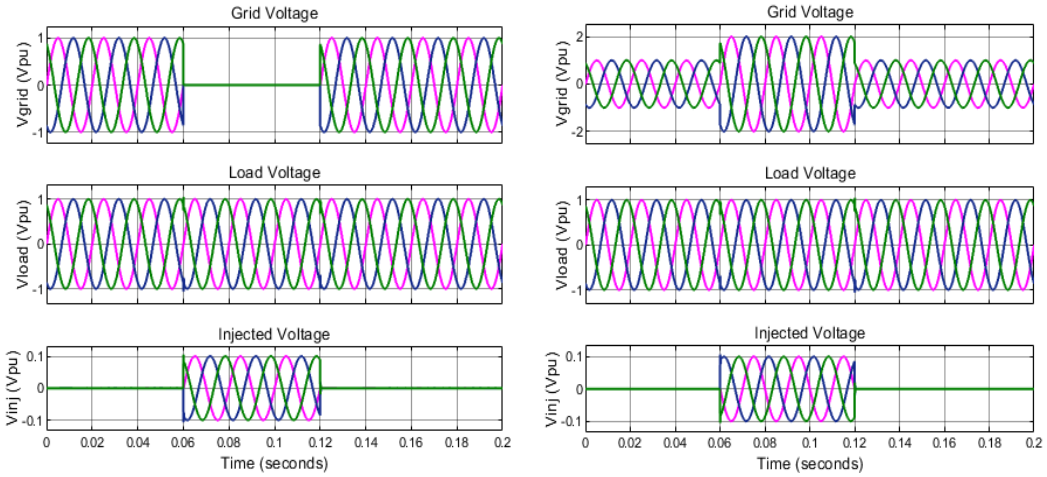

Figure 4. Simulation results of the proposed system at (a) 100% sag condition and (b) 100% swell condition

Table 2. THD analysis using load voltages at sag/swell conditions

Sag/swell	Phase -A	Phase -B	Phase -C	Avg.
No sag/swell	0.01	0.01	0.01	0.01
50%	0.02	0.86	0.87	0.59
100%	0.03	1.73	1.74	1.16

Table 3. Voltage and THD analysis of the proposed system under various fault conditions

Fault between phases (a, b, c) and ground	Voltages (Vpu)		THD (%) analysis			
	Load	Injected	Phase -A	Phase -B	Phase -C	Avg.
A	0.998	0.09984	1.13	0.01	0.01	0.384
B	0.998	0.09983	0.01	1.13	0.02	0.386
C	0.998	0.09981	0.01	0.03	2.38	0.806
AB	0.998	0.09985	1.13	1.25	0.02	0.8
BC	0.997	0.077	0.02	1.13	2.38	1.17
AC	0.996	0.079	1.13	0.03	2.38	1.18
ABC	0.998	0.09982	1.13	1.13	2.38	1.55

The fault between phase-AB and ground is introduced in the simulation between 0.06 and 0.12 seconds. Figure 5(a) illustrates the DVR technique with a PI controller at fault (phase-AB and ground), with three voltages (grid, load, and injected). To compensate for the load voltages in the grid-connected solar PV system in the event of a fault, an injected voltage of 0.09985 Vpu is obtained at phase AB. Similarly, Figure 5(b) depicts the fault situation (phase-ABC and ground) results utilizing the DVR approach. Between 0.06 and 0.12 seconds, phase-ABC's grid voltage is set to zero. To compensate for the load voltages in the grid-connected solar PV system in the event of a fault, an injected voltage of 0.09982 Vpu is obtained at phase ABC. The DVR response time of 50% and 100% sag/ swell conditions is 0.45 ms and 0.5 ms, respectively. Similarly, the average DVR response time of 0.43 ms, 0.56 ms, and 0.8 ms for the single-phase fault, the two-phase fault, and the three-phase fault in the proposed system.

Table 3 additionally tabulates the performance assessment of the percentage THD examination of the three-phase load voltage utilizing the DVR approach at different fault scenarios. After fault condition adjustments, the three-phase load voltage's percentage THD is determined. After compensation, the THD for

single-phase faults such as those at A, B, and C is 1.13 (phase-A), 1.25 (phase-B), and 2.38 (phase-C) for load voltages. After adjustment, the average THD for two-phase faults, such as those at AB, BC, and AC, is 0.8, 1.17, and 1.18 for load voltages. After adjustment, the average THD for the three-phase fault-like fault at ABC is 1.55 for load voltages. Wherever faults occur at different phases, the THD is always high. The average THD for single-, two-, and three-phase fault circumstances is 0.525, 1.05, and 1.55, respectively.

Figure 6 displays a graphic depiction of the percentage THD of load voltages during voltage disturbances. IEEE 519 requirements are met by the voltage disturbances, such as sag, swell, and fault circumstances. The FT mechanism with DVR compensates for all disturbances and satisfies IEEE 519 criteria for THD of less than 5%. The sag/swell -50 % using phase-C, sag/swell -100 % using phase-C, fault @ AB using phase-B, and fault @ ABC using phase-A are illustrated in Figure 6.

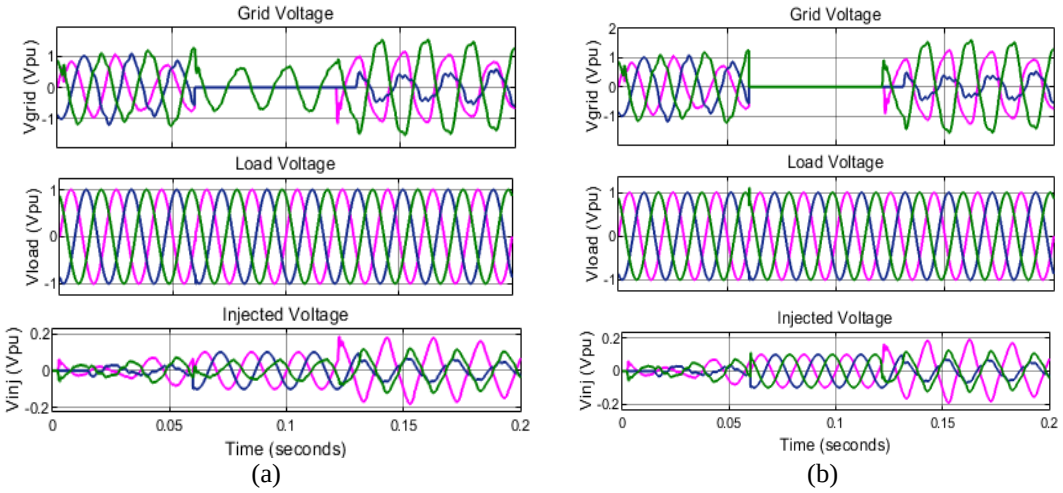

Figure 5. Simulation results of the proposed system: (a) fault @ AB and (b) fault @ ABC conditions

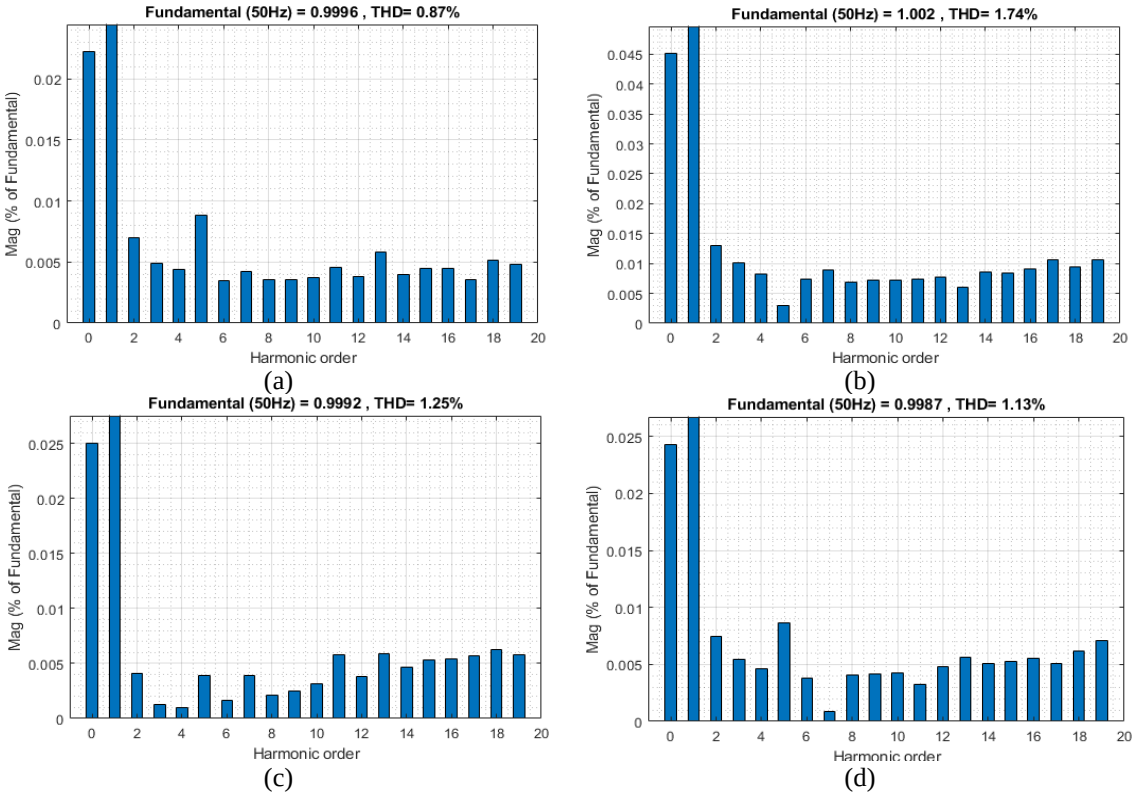

Figure 6. Representation of THD analysis: (a) sag/swell -50 % (phase-C), (b) sag/swell -100 % (phase-C), (c) fault @ AB (phase-B), and (d) fault @ ABC (phase-A)

A performance comparison of the suggested DVR-based fault-tolerant grid-connected solar PV system and other current solar PV compensating strategies documented in the literature is shown in Table 4. Parameters, including the compensation strategy, controller type, disturbance condition, and matching THD levels, are all taken into account in the comparison. A UPQC with FLC control was used in design [28], which produced THD values of 1.32% in sag, 1.08% in swell, and 2.52% in fault circumstances. Setty *et al.* [29] employed a DVR with THD varying from 1.55% to 2.12% that was regulated using PI and P + FLC techniques. To achieve 1.2% THD under mixed sag/swell conditions, Nallaiyagounder *et al.* [30] constructed a STATCOM with a multilayer discrete noise-eliminating second-order generalized integrator (MDNESOGI). Sridhar *et al.* [22] reported 2.34% THD under swell and 2.27% under sag after optimizing system stability using an MNN-PI controller. THD of 2.27% was obtained by [23] using a proportional-resonant (PR) -based current controller, while 1.1% was obtained by [25] using a shunt active power filter (S-APF) based on the AOS-FAT technique. When UPQC was used for combined sag/swell circumstances, a study in [31] produced a greater THD of 2.9%. The suggested DVR-PI-controlled system, in contrast, performs better and has the smallest average THD values, measuring 1.16% under sag/swell and 1.55% under fault conditions. In terms of control accuracy and compensation efficiency, this shows that the suggested method outperforms current methods while effectively maintaining voltage stability, minimizing harmonic distortion, and adhering to IEEE 519 criteria.

Table 4. Performance comparison of the proposed work with existing solar PV system approaches

Designs/year	System	Compensation approach	Controller	Disturbance type	THD (%)
[28], 2022	Solar PV	UPQC	FLC	Sag	1.32
				Swell	1.08
				Fault	2.52
[29], 2023	Solar PV (200 W)	DVR	PI	Sag	2.12
				Swell	2.11
			P I+ FLC	Sag	1.55
				Swell	1.54
[30], 2024	Solar PV	STATCOM	MDNESOGI	Sag/swell	1.2
[22], 2025	Solar PV (1 kW)	Optimization approach	MNN-PI	Sag	3
				Swell	2
[23], 2025	Solar PV (1 kW)	Current controller	PR	Sag	2.27
[25], 2025	Solar PV (12 kW)	Shunt active power filter (S-APF)	AOS-FAT	Sag	1.1
			FLC	Sag	2
[31], 2025	Solar PV	UPQC	NA	Sag/swell	2.9
This work	Solar PV (200 W)	DVR	PI	Sag	1.16
				Swell	1.16
				Fault	1.55

3.1. Discussion

The suggested grid-connected solar-photovoltaic system with a DVR shows exceptional voltage stability and harmonic suppression under a variety of grid disturbances. In contrast to passive mitigation techniques that only absorb or filter harmonics, the DVR uses a series-connected VSI to dynamically inject compensatory voltages in real-time, therefore bringing the load voltage back to its nominal level. The DVR maintains a steady load voltage during voltage sag situations by detecting the amplitude reduction and promptly providing a compensating voltage in phase with the source. Even at 100% sag, this active compensation method reduces power quality degradation, as seen by the low THD of 0.59% to 1.16%. The feed-forward control structure of the DVR and the quick response of the PI controller, which guarantee seamless modulation index modification without overshoot or delay, are responsible for the high-performance during sag occurrences. The DVR suppresses overvoltage at the load by injecting a voltage that is 180° out of phase with the excess supply voltage during voltage swell disturbances. Waveform integrity and a steady voltage amplitude are the outcomes of this. The system's dependability under intermittent grid situations is confirmed by the voltage waveform symmetry and harmonic content, which stay well within IEEE 519 bounds in both sag and swell circumstances.

The DVR's performance is still strong in fault situations, particularly in two- and three-phase-to-ground faults, with THD only slightly increasing (up to 1.55%). This happens as a result of the DVR actively correcting the phase angle variation caused by the uneven grid voltages in addition to compensating for the voltage magnitude. The incorporation of a PWM inverter with fast switching capacity guarantees quick compensation and harmonic isolation, while the simplicity of the PI controller facilitates real-time adjustment. The suggested DVR system yields a lower THD than more sophisticated control strategies like fuzzy logic, neural networks, or PR controllers when compared to the results of recent research (Table 4). This illustrates that excellent compensation accuracy can be attained by the DVR's streamlined control loop

without the need for highly computational optimization. The results are consistent with research by [28] and [30], which highlighted that dynamic compensators are more effective than static VAR and filter-based systems at preserving grid stability when renewable generation fluctuates. The proposed DVR-integrated PV system's fast transient response, strong harmonic rejection, and phase-compensated voltage injection all contribute to its overall superior performance, which guarantees continuous load power quality even in the event of grid anomalies. Its fault-tolerant and appropriateness for dispersed renewable networks, where grid conditions are often less than perfect, are both confirmed by the study.

4. CONCLUSION

An effective grid-connected solar PV system with a fault-tolerant (FT) mechanism that uses a DVR to reduce grid-side voltage disturbances like sag, swell, and fault conditions was presented in this study. A 200 W Waaree Energies WSM-315 module, a VSC-based DC–DC converter, and an MPPT controller with the P&O algorithm were used in the system to guarantee stable operation and ideal power extraction. The suggested DVR-based FT control successfully corrected for voltage variations, according to simulation findings, obtaining THD values well within the IEEE 519 limit of 5%—1.16% under sag/swell and 0.525%, 1.05%, and 1.55% under single-, two-, and three-phase faults, respectively. The innovation is in including a quick and lightweight DVR control mechanism that improves reliability, lowers harmonic distortion, and increases voltage stability without requiring intricate calculations. For distributed renewable networks, the solution provides improved power quality and affordable voltage adjustment. It is restricted to simulation-based validation, though, and more research into hardware performance, controller latency, and real-time viability is required.

The suggested fault-tolerant grid-connected solar PV system with a DVR base efficiently reduces voltage fluctuations and keeps THD within IEEE 519 bounds. However, without hardware-in-the-loop (HIL) or real-time implementation, the study is restricted to simulation-based validation. Future research should investigate integration with smart inverters or grid-forming converters for improved grid support, as well as controller latency, sampling rate, and embedded practicality using FPGA or DSP-based platforms. A more realistic evaluation would be obtained by expanding the existing model to include hybrid sag/swell–fault situations as well as renewable-rich or weak-grid settings, as it now concentrates on individual disturbances. Dynamic tuning and fault recovery speed could be further enhanced by integrating fault classification and adaptive control using AI-driven techniques (ANN, ANFIS). It is advised that research be done at the grid level on the best way to deploy DVRs, coordinate distributed PV systems, and adhere to national PQ standards. Furthermore, practical applicability will be strengthened through examination of switching losses, thermal stress, and economic viability. Overall, the system's preparedness for smart-grid integration and the improvement of renewable energy stability will be advanced by moving toward real-time, adaptable, and scalable DVR control mechanisms.

FUNDING INFORMATION

Authors state no funding involved.

AUTHOR CONTRIBUTIONS STATEMENT

This journal uses the Contributor Roles Taxonomy (CRediT) to recognize individual author contributions, reduce authorship disputes, and facilitate collaboration.

Name of Author	C	M	So	Va	Fo	I	R	D	O	E	Vi	Su	P	Fu
N. Jayakumar	✓	✓	✓	✓	✓	✓		✓	✓	✓			✓	
B. Devi Vighneshwari		✓				✓		✓	✓	✓	✓	✓		
V. Prema		✓	✓	✓		✓		✓	✓			✓		

C : **C**onceptualization
M : **M**ethodology
So : **So**ftware
Va : **Va**lidation
Fo : **Fo**rmal analysis
I : **I**nvestigation
R : **R**esources
D : **D**ata Curation
O : Writing - **O**riginal Draft
E : Writing - Review & **E**diting
Vi : **Vi**sualization
Su : **Su**pervision
P : **P**roject administration
Fu : **Fu**nding acquisition

CONFLICT OF INTEREST STATEMENT

Authors state no conflict of interest.

DATA AVAILABILITY

The data that support the findings of this study are available from the corresponding author, [NJ], upon reasonable request.

REFERENCES

[1] Z. M. Alaas, "The effects of temperature on photovoltaic and different mitigation techniques: a review," *IEEE Access*, vol. 12, pp. 180309–180327, 2024, doi: 10.1109/ACCESS.2024.3504009.

[2] M. Jalal, I. U. Khalil, A. U. Haq, A. Flah, and S. A. M. Abdel Wahab, "Advancements in PV array reconfiguration techniques: review article," *IEEE Access*, vol. 12, pp. 183751–183778, 2024, doi: 10.1109/ACCESS.2024.3509955.

[3] P. Singh, U. Kumar, N. K. Choudhary, and N. Singh, "Advancements in protection coordination of microgrids: a comprehensive review of protection challenges and mitigation schemes for grid stability," *Protection and Control of Modern Power Systems*, vol. 9, no. 6, pp. 156–183, Nov. 2024, doi: 10.23919/PCMP.2023.000250.

[4] X. Liang and C. Andalib -Bin- Karim, "Harmonics and mitigation techniques through advanced control in grid-connected renewable energy sources: a review," *IEEE Transactions on Industry Applications*, vol. 54, no. 4, pp. 3100–3111, Jul. 2018, doi: 10.1109/tia.2018.2823680.

[5] N. Saxena, I. Hussain, B. Singh, and A. L. Vyas, "Implementation of a grid-integrated PV-battery system for residential and electrical vehicle applications," *IEEE Transactions on Industrial Electronics*, vol. 65, no. 8, pp. 6592–6601, Aug. 2018, doi: 10.1109/TIE.2017.2739712.

[6] A. K. Singh, I. Hussain, and B. Singh, "Double-stage three-phase grid-integrated solar PV system with fast zero attracting normalized least mean fourth based adaptive control," *IEEE Transactions on Industrial Electronics*, vol. 65, no. 5, pp. 3921–3931, May 2018, doi: 10.1109/tie.2017.2758750.

[7] E. Lorenzani, G. Migliazza, F. Immovilli, C. Gerada, H. Zhang, and G. Buticchi, "Internal current return path for ground leakage current mitigation in current source inverters," *IEEE Access*, vol. 7, pp. 96540–96548, 2019, doi: 10.1109/access.2019.2929062.

[8] V. N. Kumar, N. Babu P., R. Kiranmayi, P. Siano, and G. Panda, "Improved power quality in a solar PV plant integrated utility grid by employing a novel adaptive current regulator," *IEEE Systems Journal*, vol. 14, no. 3, pp. 4308–4319, Sep. 2020, doi: 10.1109/jsyst.2019.2958819.

[9] A. Kulkarni and V. John, "Mitigation of lower order harmonics in a grid-connected single-phase PV inverter," *IEEE Transactions on Power Electronics*, vol. 28, no. 11, pp. 5024–5037, Nov. 2013, doi: 10.1109/tpel.2013.2238557.

[10] Y. Yang, K. Zhou, and F. Blaabjerg, "Current harmonics from single-phase grid-connected inverters—examination and suppression," *IEEE Journal of Emerging and Selected Topics in Power Electronics*, vol. 4, no. 1, pp. 221–233, Mar. 2016, doi: 10.1109/jestpe.2015.2504845.

[11] A. Moghassemi, S. Padmanaban, V. K. Ramachandaramurthy, M. Mitolo, and M. Benbouzid, "A novel solar photovoltaic fed TransZSI-DVR for power quality improvement of grid-connected PV systems," *IEEE Access*, vol. 9, pp. 7263–7279, 2021, doi: 10.1109/access.2020.3048022.

[12] P. Shah and B. Singh, "Kalman filtering technique for rooftop-PV system under abnormal grid conditions," *IEEE Transactions on Sustainable Energy*, vol. 11, no. 1, pp. 282–293, Jan. 2020, doi: 10.1109/tste.2018.2890600.

[13] R. K. Varma and S. Mohan, "Mitigation of fault induced delayed voltage recovery (FIDVR) by PV-STATCOM," *IEEE Transactions on Power Systems*, vol. 35, no. 6, pp. 4251–4262, Nov. 2020, doi: 10.1109/tpwrs.2020.2991447.

[14] H. P. Lee, K. Dsouza, K. Chen, N. Lu, and M. E. Baran, "Adopting dynamic VAR compensators to mitigate PV impacts on unbalanced distribution systems," *IEEE Access*, vol. 11, pp. 101514–101524, 2023, doi: 10.1109/access.2023.3315601.

[15] M. I. Nazir *et al.*, "Techno-economic and sensitivity analysis of grid connected perovskite PV-wind systems," *IEEE Access*, vol. 12, pp. 78397–78408, 2024, doi: 10.1109/access.2024.3408239.

[16] S. Bagherwal and S. Mahapatra, "Enhanced stability and control of solar powered EV charging stations using disturbance observer-based adaptive sliding mode control for DC voltage stabilization," *IEEE Access*, vol. 12, pp. 183293–183311, 2024, doi: 10.1109/access.2024.3511637.

[17] P. R. Bana, S. D'Arco, and M. Amin, "ANN-based robust current controller for single-stage grid-connected PV with embedded improved MPPT scheme," *IEEE Access*, vol. 12, pp. 100251–100262, 2024, doi: 10.1109/access.2024.3429347.

[18] I. Hassan *et al.*, "Explainable deep learning model for grid-connected photovoltaic system performance assessment for improving system reliability," *IEEE Access*, vol. 12, pp. 120729–120746, 2024, doi: 10.1109/access.2024.3452778.

[19] A. Radwan, M. A. Elshenawy, Y. A.-R. I. Mohamed, and E. F. El-Saadany, "Grid-forming voltage-source inverter for hybrid wind-solar systems interfacing weak grids," *IEEE Open Journal of Power Electronics*, vol. 5, pp. 956–975, 2024, doi: 10.1109/ojpel.2024.3410908.

[20] Z. Guo and W. Wu, "Matching synchronous machine control for improving active support of grid-forming PV systems with enhanced DC voltage dynamics," *Journal of Modern Power Systems and Clean Energy*, vol. 13, no. 1, pp. 179–189, 2024, doi: 10.35833/mpce.2023.000624.

[21] M. Mohamed, Z. M. Alaas, B. Al Faiya, H. Y. Hegazy, W. I. Mohamed, and S. A. M. Abdelwahab, "Performance improvement of grid-connected PV-wind hybrid systems using adaptive neuro-fuzzy inference system and fuzzy FOPID advanced control with OPAL-RT," *IEEE Access*, vol. 13, pp. 55996–56020, 2025, doi: 10.1109/access.2025.3548926.

[22] B. Sridhar *et al.*, "Design and analysis of modular neural network-based PI-controller ensemble with karush-kuhn-tucker conditions for grid-connected photovoltaic systems under ground fault conditions," *IEEE Access*, vol. 13, pp. 67196–67219, 2025, doi: 10.1109/access.2025.3559139.

[23] M. Karimi and A. Khaki-Sedigh, "Design and implementation of solar grid-connected inverter with the approach of maximum power injection and THD reduction in partial shading conditions using cascaded repetitive controller," *IEEE Access*, vol. 13, pp. 48923–48934, 2025, doi: 10.1109/access.2025.3533602.

[24] M. F. Kibria *et al.*, "A hybrid single-phase transformerless solar photovoltaic grid-connected inverter with reactive power capability and reduced leakage current," *IEEE Access*, vol. 13, pp. 39235–39247, 2025, doi: 10.1109/access.2025.3546670.

[25] B. Kiruthiga, R. Karthick, I. Manju, and K. Kondreddi, "Optimizing harmonic mitigation for smooth integration of renewable energy: a novel approach using atomic orbital search and feedback artificial tree control," *Protection and Control of Modern Power Systems*, vol. 9, no. 4, pp. 160–176, Jul. 2024, doi: 10.23919/pcmp.2023.000577.

[26] Y. Wesseling, N. Damianakis, G. Ram Chandra Mouli, and P. Bauer, "Grid impact of unbalanced phase integration of PV generation, electrified mobility, and heating in LV distribution grids," *IEEE Access*, vol. 13, pp. 56887–56907, 2025, doi: 10.1109/access.2025.3555169.
[27] M. S. Bhaskar, S. R. Vemparala, D. Almakhles, K. S., and M. F. Elmorshedy, "A scalable high-voltage gain DC/DC converter with reduced voltage stress for DC microgrid integration," *IEEE Open Journal of the Industrial Electronics Society*, vol. 6, pp. 277–289, 2025, doi: 10.1109/ojies.2025.3536032.
[28] H. Kenjrawy, C. Makdisie, I. Houssamo, and N. Mohammed, "New modulation technique in smart grid interfaced multilevel UPQC-PV controlled via fuzzy logic controller," *Electronics*, vol. 11, no. 6, p. 919, Mar. 2022, doi: 10.3390/electronics11060919.
[29] S. N. Setty, M. S. D. Shashikala, and K. T. Veeramanju, "Hybrid control mechanism-based DVR for mitigation of voltage sag and swell in solar PV-based IEEE 33 bus system," *International Journal of Power Electronics and Drive Systems (IJPEDS)*, vol. 14, no. 1, pp. 209–221, Mar. 2023, doi: 10.11591/ijpeds.v14.i1.pp209-221.
[30] K. Nallaiyagounder, V. Madhaiyan, R. Murugesan, and O. Aldosari, "Photovoltaic-based q-ZSI STATCOM with MDNESOGI control scheme for mitigation of harmonics," *Energies*, vol. 17, no. 2, p. 534, Jan. 2024, doi: 10.3390/en17020534.
[31] J. S. Espinosa Gutiérrez and A. Aguila Téllez, "Optimal placement of a unified power quality conditioner (UPQC) in distribution systems using exhaustive search to improve voltage profiles and harmonic distortion," *Energies*, vol. 18, no. 17, p. 4499, Aug. 2025, doi: 10.3390/en18174499.

BIOGRAPHIES OF AUTHORS

N. Jayakumar received his B.E. in Electrical and Electronics Engineering from Bharathidasan University, Tamil Nadu, in 2001 and received his M.Tech. in Power Electronics and Drives from SASTRA University, Thanjavur (TN) in 2005. He is currently working as an assistant professor at the department of Electrical and Electronics Engineering in The Oxford College of Engineering, Bangalore. His research includes power electronics converters, electric vehicles. He has published papers in international journals and conferences in the area of power electronics. He is a life member of ISTE. He can be contacted at email: jayakumar.toce@gmail.com.

Dr. B. Devi Vighneshwari is professor and head of the Department of Electrical & Electronics Engineering at The Oxford College of Engineering, Bangalore. She holds a B.E., M.E., and Ph.D. from Annamalai University in the field of Electrical & Electronics Engineering, and has over 20 years of teaching experience, and has published various papers in international journals & conferences. Her area of research interest is power quality, smart grid, microcontroller, power systems, and IoT. She is a life member of ISTE. She can be contacted at email: devivighneshwari@gmail.com.

Dr. V. Prema received the B.Tech. and M.Tech. degrees in electrical engineering and Power Electronics from Calicut University and Visvesvaraya Technological University, respectively. She received the Ph.D. degree in electrical engineering from Visvesvaraya Technological University in the area of Hybrid Microgrid. She has 20 years of teaching and industry experience. Currently, she is working as an associate professor at B.M.S. College of Engineering, Bangalore, India. She has authored more than 25 articles in various journals and conferences. She is a senior member of IEEE, IEEE Industrial Electronics, and Power Electronics. She is a reviewer member of various international journals and conferences. Her research interests include renewable energy, microgrids, and power electronics. She can be contacted at email: premav.eee@bmsce.ac.in.